Nonlinear Interaction between a Frequency Signal and Neighboring Data Channels in a Commercial Optical Fiber Communication System

by

Patrick Sykes

Table of Contents

Chapter 1: Introduction

Improvements in optical frequency references allow them to be more precise than current atomic clock standards at microwave frequencies [1–3]. It is expected that this greater precision will ultimately lead to a redefinition of the second, and greater precision and accuracy in timekeeping [2]. It is desirable for many applications to transmit time and frequency from highly accurate and precise references, like those at the National Institute of Standards and Technology or the US Naval Observatory, to distant locations. However, the transmission medium distorts the time and frequency data – degrading their accuracy and precision.

Accurate timekeeping is required in the Global Positioning System (GPS) satellites and receivers, transaction logging, and research experiments [4]. Currently, there are techniques and systems for time and frequency transfer in wireless communication systems. A common method is the two-way satellite time and frequency transfer system, which enables two laboratories to use a satellite as a common link to synchronize their clocks. These wireless systems are typically accurate to within $1 - 10$ ns [5], which is sufficient for many applications, but far less accurate than the best primary references [6,

7]. Additionally, satellites are physically inaccessible, which makes hardware maintenance and upgrades difficult and the satellites themselves vulnerable to attack. Fiber optics are a potential substitute for land-based transfer, especially if one can take advantage of the existing fiber telecommunications infrastructure.

Research networks are increasingly transmitting time and frequency signals along with data over fiber optic communication systems. These networks include the Réseau Fibré Métrologique à Vocation Européenne (REFIMEVE+) in France [8], PIONIER in Poland [9], and the White Rabbit networks used at the CERN accelerator sites and GSI's Facility for Antiproton and Ion Research [10]. A larger European optical time and frequency distribution network called CLONETS is planned [11]. The REFIMEVE+ project has demonstrated frequency transfer over optical fibers with a stability of 10^{-16} at 1 s and 10^{-19} at 10^4 s over a distance of 1480 km [8]. These systems place the frequency signal in a frequency channel that is used for data transmission.

In a typical optical communication system, there are many data channels centered at different optical wavelengths, which is a technique called wavelength division multiplexing (WDM). Each channel has some finite bandwidth so that they do not overlap in the frequency domain. In this thesis, we will be considering the possibility of transmitting a frequency signal in the interstices of the WDM channels. We will examine the limits that fiber impairments impose on this frequency signal in a long-haul system. A number

of different physical effects impair signal transmission in optical fibers [12]. Signal impairments include amplified spontaneous emission (ASE) noise from amplifiers, dispersion, and the Kerr nonlinearity [12]. Scattering nonlinearities due to the Rayleigh, Brillouin, and Raman effects, can also impair the signal [12, 13]. Preliminary work indicates that this frequency signal can be transmitted with both a narrow bandwidth ($\lesssim$ 100 MHz) and low power ($\lesssim 10\ \mu$W) compared to a data channel [14]. The bandwidth of a data channel in a long-haul system is typically $10-100$ GHz [15], while a typical power in a terrestrial long-haul system for a WDM channel is 0 dBm (1 mW) at the transmitter and less than -10 dBm (0.1 mW) prior to an amplifier as the signal attenuates. In this case, the most important impairment that the frequency signal suffers is due to cross-phase modulation between the frequency signal and the neighboring data channels. In this thesis, we will quantify the impact of cross-phase modulation on the frequency signal and determine the limits that it imposes.

The individual data channels are modulated to transmit information. Modulation formats are on-off keying (OOK), binary phase shift keying (BPSK), quadrature phase shift keying (QPSK), and differential phase shift keying (DPSK) [12]. An OOK signal is the simplest modulation format. A binary 0 is represented by the absence of power in a time slot and a binary 1 is represented by some non-zero power that is sufficiently large so that noise does not lead to an acceptable probability of confusing 0's and 1's. There cannot be a sharp transition from a 0 to a 1 and vice versa because a com-

munication channel can only occupy a limited bandwidth. In practice, each bit occupies a time slot where its value is held for a short time. The signal can start building up to a 1 from a 0 in the preceding time slot and then decay back to a 0 in the following time slot. Thus, the physical representation of the bits overlaps with neighboring bits, and the amount of overlap is characterized by a roll-off parameter. This overlap can lead to intersymbol interference [16].

A frequency signal has periodic zero crossings. However, fiber impairments can alter the timing of the zero crossings. These phase shifts broaden the frequency that is transmitted so that it is no longer a pure tone. We will show that the most important optical impairment is due to cross-phase modulation between a frequency signal and neighboring data channels. We must find the distribution of the amplitude of the data channels in order to calculate their variance and their impact on the variance of the frequency signal. The distribution of the amplitude of the channel is mainly influenced by dispersion. We calculate the effect of dispersion on an OOK signal, and we then calculate the variance of the data channel intensities as a function of distance. Given this variance, we can then calculate the phase and frequency variance of the frequency channel.

Chapter 2 introduces methods for measuring the frequency stability of oscillators. We present the reasoning behind formulating different time stability measures, and issues with some of the usual statistical measures, such as the mean and variance, that were developed for treating stationary pro-

cesses. We reveal the relations between each of the methods. We focus in particular on the second structure function and Allan deviation for the measure of phase and frequency stability, respectively.

Chapter 3 is an overview of the common impairments a signal experiences in an optical fiber. The impairments will affect both a data channel and the frequency signal. Here the limits of the impairments will be investigated. These impairments determine the power and frequency requirements for the frequency signal. After eliminating the negligible impairments, we demonstrate that cross-phase modulation is the principal non-environmental source of frequency spread in the frequency channel.

Chapter 4 describes the phase noise computations. We perform statistical and time stability analyses on the phase noise to determine the variance of the frequency fluctuations.

Chapter 5 concludes the thesis.

Chapter 2: Phase and Frequency Stability Measures

2.1 Introduction

Timekeeping requires a periodic event that can be counted and a time reference point. In order to synchronize two clocks, it is necessary to match the frequency of the periodic event and transfer the reference point. Figuring out the reference point requires calculating an approximate delay due to propagation, which can be achieved by transmitting a time point and then waiting to receive confirmation from the other system. The White Rabbit Project achieves synchronization by using Synchronous Ethernet for syntonization, and the IEEE 1588 Precision Time Protocol [10] to determine the initial time point.

However, no frequency source is perfect; there are initialization errors, manufacturing flaws, and environmental influences. Environmental sources for oscillator instability include pressure, temperature, and magnetic fields [17]. This thesis investigates the instabilities caused by optical impairments from the fiber medium and amplifiers. Environmental effects or issues inherent to the oscillator source have been treated in other studies [17–19].

A frequency source can be represented as

$$u_c(t) = [U_0 + \epsilon(t)] \sin[\omega_0 t + \phi(t)] \tag{2.1}$$

where U_0 is the amplitude and $\epsilon(t)$ is amplitude fluctuation. The quantity ω_0 is the nominal angular frequency, and $\phi(t)$ is the phase fluctuation. The amplitude fluctuation is much less than the nominal amplitude, $|\epsilon(t)| \ll |U_0|$, and the frequency fluctuation, given by the time derivative of the phase, $\dot{\phi} \equiv d\phi/dt$, must be much less than the nominal angular frequency, $|\dot{\phi}| \ll |\omega_0|$. Otherwise, the frequency signal is too heavily distorted to be useful.

The instantaneous frequency is defined as the time derivative of the total phase

$$\omega(t) = \frac{d}{dt} [\omega_0 t + \phi(t)] = \omega_0 + \dot{\phi}(t). \tag{2.2}$$

Most of the literature on time and frequency control uses the fractional frequency, $y(t)$, and the phase time, $x(t)$, [20–22]

$$y(t) = \frac{\omega(t) - \omega_0}{\omega_0} = \frac{\dot{\phi}(t)}{\omega_0}, \qquad x(t) = \int_0^t y(\tau) d\tau = \frac{\phi(t)}{\omega_0}. \tag{2.3}$$

However, it is useful for our theoretical study to work mainly with ϕ and $\dot{\phi}$. Using ϕ and $\dot{\phi}$ emphasizes the phase and frequency deviations of the signal and is more convenient in theoretical work, whereas the fractional frequency and phase time are better suited for physical measurements. Note also that x and ϕ are measured instantaneously, while measuring y requires a time

average

$$\bar{y}_k = \frac{1}{\tau}\int_{t_k}^{t_k+\tau} y(t)dt. \tag{2.4}$$

The invention of atomic clocks necessitated a means of quantifying frequency stability [21, 23]. Since the errors have a random component, the use of statistical measures like the power spectral density (PSD) is necessary. In general, the variations in time and frequency measurements can not be described as a stationary process and defining a variance in the usual sense is not possible [17, 21]. This difficulty led to the invention of the Allan variance [17, 21]. Structure functions are another approach to characterising phase and frequency variation [24]. In this chapter, we will describe these different approaches and then show the relationships among them.

2.2 Power Spectral Density

The PSD of the phase noise can be obtained by feeding the output of a phase demodulator into a spectrum analyser, and, similarly, the PSD of the frequency noise can be obtained by feeding the output of a frequency demodulator into a spectrum analyzer [17].

For any of the quantities $w = x$, y, ϕ, or $\dot{\phi}$ the autocorrelation is defined as

$$R_w(\tau) = E\{w(t)w(t+\tau)\} = \lim_{T\to\infty}\frac{1}{T}\int_0^T w(t)w(t+\tau)dt \tag{2.5}$$

and the corresponding PSDs are the Fourier transforms of the autocorrelations

$$S_w(\omega) = 2\int_0^\infty R_w(\tau)\cos(\omega\tau)d\tau \tag{2.6}$$

$$R_w(\tau) = \frac{1}{\pi}\int_0^\infty S_w(\omega)\cos(\omega\tau)d\omega \tag{2.7}$$

Evaluating $R_w(\tau)$ at $\tau = 0$ gives us the second moment of w,

$$R_w(0) = E\{[w(t)]^2\} = \int_0^\infty S_w(\omega)d\omega$$

which we refer to as the signal power. If we compare the PSD of two different sources, then the one with the lower signal power will typically have less error.

The PSDs for each of our quantities are related. We find

$$S_{\dot{\phi}}(\omega) = \omega^2 S_\phi(\omega), \tag{2.8}$$

$$S_y(\omega) = \frac{\omega^2}{\omega_0^2} S_\phi(\omega), \tag{2.9}$$

$$S_x(\omega) = \frac{1}{\omega_0^2} S_\phi(\omega). \tag{2.10}$$

Oscillator noise can typically be decomposed into a power series $S_\phi(\omega) = \sum_{k=0}^{4} h_k \omega^{-k}$ [22]. The term proportional to ω^0 is referred to as white phase noise, the ω^{-1} term is referred to as flicker phase noise, and ω^{-2} is referred to as random walk phase noise. Since $S_{\dot{\phi}}(\omega) = \omega^2 S_\phi(\omega)$, the powers in the series increase by 2. The term proportional to ω^{-3} term is

referred to as flicker frequency noise, and the term proportional to ω^{-4} as random walk frequency noise [6, 20, 25, 26].

2.3 Allan Variance

The distribution of frequency error is difficult to determine because the error is typically nonstationary. The sample variance from finitely many measurements may not converge to the true variance of the process as the number of samples goes to infinity. The Allan Variance is the mean of sample variances calculated over an interval. The definition is based on the fractional frequency y and phase time x, however we will express it in terms of the phase ϕ. We use the averaged quantity $\bar{y}_k$ defined in eq. 2.4.

The N-sample mean is defined as

$$\mu = \frac{1}{N}\sum_{k=1}^{N} \bar{y}_k. \tag{2.11}$$

The N-sample mean can then be used for the N-sample variance,

$$\sigma_S^2(N) = \frac{1}{N-1}\sum_{k=1}^{N} (\bar{y}_k - \mu)^2 = \frac{1}{N-1}\sum_{k=1}^{N} \left(\bar{y}_k - \frac{1}{N}\sum_{i=1}^{N} \bar{y}_i\right)^2. \tag{2.12}$$

The Allan variance [21] is the mean of the sample variances over all time.

$$\sigma_A^2(N,\tau) = \langle \sigma_S^2(N) \rangle = \left\langle \frac{1}{N-1}\sum_{k=1}^{N} \left(\bar{y}_k - \frac{1}{N}\sum_{i=1}^{N} \bar{y}_i\right)^2 \right\rangle \tag{2.13}$$

In general, the Allan variance utilises N samples, where N can have any integer value greater than 1, but typically the $N = 2$ two-sample Allan variance is used, for which

$$\sigma_A^2(2,\tau) = \frac{1}{2}\langle[\bar{y}_{k+1} - \bar{y}_k]^2\rangle. \tag{2.14}$$

It is not possible to average over all time so one computes the Allan variance from a set of M total samples, so that

$$\sigma_A^2(\tau, M) = \frac{1}{2(M-1)} \sum_{k=1}^{M-1} (\bar{y}_{k+1} - \bar{y}_k)^2 \tag{2.15}$$

where it is understood that $N = 2$ in the definition of $\sigma_A^2(\tau, M)$. The averaged fractional frequency is related to the phase by the relationship $\bar{y}_k = [\phi(t_k + \tau) - \phi(t_k)]/(\omega_0\tau)$. Hence, the Allan variance may be written in terms of the phase as

$$\sigma_A^2(\tau) = \frac{1}{2}\left\langle \left[\frac{\phi(t_k + 2\tau) - \phi(t_k + \tau)}{\omega_0\tau} - \frac{\phi(t_k + \tau) - \phi(t_k)}{\omega_0\tau}\right]^2 \right\rangle. \tag{2.16}$$

2.4 Structure Functions

The structure functions are based off of studies that Kolmogorov performed on turbulence [24]. The oscillator phase $\phi(t)$ can be written as the process

$$\phi(t) = \omega_0 t + \sum_{k=2}^{N} \frac{\Omega_{k-1}}{k!} t^k + \psi(t) + \phi_0 \tag{2.17}$$

where $\psi(t)$ is the short-term phase fluctuation, which can be considered stationary, and ϕ_0 is a constant. The remaining terms take into account the long-term phase drift. This long term drift is the source of nonstationarity. The structure functions can be used to remove the long term drift from $\phi(t)$.

The first difference equation

$$\Delta\phi(\tau) := \Delta\phi(t;\tau) = \phi(t+\tau) - \phi(t) \tag{2.18}$$

is the total phase accumulated over the interval τ. The N-th difference equation is defined recursively, using

$$\Delta^N\phi(\tau) = \Delta^{N-1}\left[\Delta\phi(\tau)\right]. \tag{2.19}$$

Whenever the process $\phi(t)$ is a (wide-sense) stationary process, the mean of the N-th difference equation is 0. The N-th order structure function is then the second moment of the N-th difference equation,

$$D_\phi^{(N)}(\tau) = \langle[\Delta^N\phi(\tau)]^2\rangle. \tag{2.20}$$

Since the first difference equation is the total phase accumulation, the function $[D_\phi^{(1)}(\tau)]^{1/2}$ equals the mean phase accumulation. Dividing the first difference equation by the time difference τ is equivalent to discrete differentiation in time, so that $[\phi(t+\tau)-\phi(t)]/\tau$ is the discrete frequency accumulation over τ, and the standard deviation of this term is the mean frequency accumulation [24].

The random process need not be (wide-sense) stationary in order for the difference equation to be stationary. For example, if the process is an n-th order polynomial with an additive stationary process, then the M-th difference equation eliminates all the polynomial terms whenever $M > n$, and we are left with the M-th difference of the stationary process.

For a stationary process, there is a further simplification for the first structure function. Expanding the expectation term gives

$$\langle[\phi(t+\tau)-\phi(t)]^2\rangle = \langle\phi(t+\tau)\phi(t+\tau)+\phi(t)\phi(t)-2\phi(t+\tau)\phi(t)\rangle. \quad (2.21)$$

The first two terms on the right hand side of the equation are the variance of the process ϕ because it is stationary, and we get the simplification

$$\langle[\phi(t+\tau)-\phi(t)]^2\rangle = 2R_\phi(0)-2R_\phi(\tau) \quad (2.22)$$

where $R_\phi(\tau)$ is the autocorrelation defined in Eq. 2.5. The structure functions can be computed to higher accuracy using less data than the correlation function [27]. This advantage is particularly noticeable for "flicker" noise whose power spectral density is proportional to ω^{-1} and is commonly present

in oscillator noise.

2.5 Converting between different measures

The power spectral density (PSD) is the most fundamental measure of frequency stability. However, sampling the time data points over a sufficiently long time to accurately obtain the PSD at low frequencies can be difficult. In particular, there may not be enough frequency resolution to obtain low frequency deviations proportional to ω^{-1}, referred to as "flicker noise" [26]. When the power spectrum is available, the structure functions and the Allan variance can be obtained from it. The reverse is not generally true, although it is sometimes possible through the use of Mellin transformations [20, 24].

Allan variance to the second-order structure function:

We now show that the Allan variance is proportional to the second-order structure function. Using the definition of Allan variance in Eq. 2.16, we obtain

$$\sigma_A^2(2,\tau) = \frac{1}{2}\left\langle \left[\frac{\phi(t_k+2\tau)-\phi(t_k+\tau)}{\omega_0\tau} - \frac{\phi(t_k+\tau)-\phi(t_k)}{\omega_0\tau} \right]^2 \right\rangle \tag{2.23}$$

$$= \frac{1}{2\omega_0^2\tau^2}\langle [\phi(t_k+2\tau) - 2\phi(t_k+\tau) + \phi(t_k)]^2 \rangle. \tag{2.24}$$

The t_k are arbitrary when averaging over all time, so the ensemble average is equal to the structure function $D_\phi^{(2)}(\tau)$ divided by $2\omega_0^2$.

Power spectral density to structure functions:

The relation between the power spectral density and the structure function depends on the long term frequency drift of the oscillator and whether the M-th difference equation is stationary [24]. Suppose that the drift is compensated or $M > N$, where N is the highest-order polynomial term for the drift, then we find

$$D_{\phi}^{(M)}(\tau) = 2^{2M} \int_{-\infty}^{\infty} \sin^{2M}\left(\frac{\omega\tau}{2}\right) S_{\phi}(\omega) d\omega. \tag{2.25}$$

Power spectral density to Allan variance:

Since we demonstrated that the Allan variance is proportional to a structure function in Eq. 2.23, we combine the results from the last two sections, and we obtain

$$\sigma_A^2(2,\tau) = \frac{2^2}{\omega_0^2\tau^2} \int_{-\infty}^{\infty} \sin^4\left(\frac{\omega\tau}{2}\right) S_{\phi}(\omega) d\omega. \tag{2.26}$$

2.6 Chapter remarks

We will be using the structure functions, specifically $D_{\phi}^{(1)}(\tau)$, as our preferred measure of stability. The reason for this choice is that it requires fewer samples than the correlation to compute "flicker" noise, and it is simple to implement and interpret. We will also use the Allan deviation to characterize the stability because it is a common measure of frequency sta-

bility in the oscillator communities, and we can obtain it from the structure function $D_{\phi}^{(2)}(\tau)$. The power spectral density is preferred for experimental measurements.

Chapter 3: Optical Fiber Impairments

3.1 Introduction

Propagation through an optical fiber distorts a frequency signal. Previous work described the various optical impairments in an optical fiber and their influence on a frequency signal [14]. In this chapter, we summarize that work and relate it to our simulations.

The propagation of light through an optical fiber can be modeled using the nonlinear Schrödinger (NLS) equation [13],

$$\frac{\partial u}{\partial z} + \beta_1 \frac{\partial u}{\partial t} + \frac{i\beta_2}{2}\frac{\partial^2 u}{\partial t^2} + \frac{\alpha}{2}u = i\gamma|u|^2 u. \tag{3.1}$$

where u is the pulse envelope, β_1 is the group velocity, β_2 is the group velocity dispersion, α is the attenuation, and γ is the Kerr nonlinearity.

We split the input signal into a combination of two signals, $u = u_d \exp(-i\Delta\omega t) + u_f$. These are u_d, the data channel, and u_f, the frequency signal. It is helpful to define a reference frame moving with the frequency signal $T = t - z/v_f$, where T is the retarded time and v_f is the group velocity of the frequency signal. The data channel now travels at the difference velocity

$\delta = (v_f - v_d)/(v_f v_d)$.

The right hand side of Eq. 3.1 is nonlinear, so that the sum of the two signals must be handled produces several cross-terms,

$$\begin{aligned}
&|u_d \exp(-i\Delta\omega t) + u_f|^2 (u_d \exp(-i\Delta\omega t) + u_f) \\
&(u_d \exp(-i\Delta\omega t) + u_f)(u_d^* \exp(i\Delta\omega t) + u_f^*)(u_d \exp(-i\Delta\omega t) + u_f) \\
&= |u_d|^2 u_d \exp(-i\Delta\omega t) + 2|u_f|^2 u_d \exp(-i\Delta\omega t) + u_f^2 u_d^* \exp(i\Delta\omega t) \\
&\quad + u_d^2 u_f^* \exp(-i2\Delta\omega t) + 2|u_d|^2 u_f + |u_f|^2 u_f. \qquad (3.2)
\end{aligned}$$

We can now split Eq. 3.1 into two differential equations based on matching their phase terms,

$$\frac{\partial u_f}{\partial z} + \frac{\alpha_f}{2} u_f + \frac{i\beta_{2f}}{2} \frac{\partial^2 u_f}{\partial T^2} = i\gamma_f \left(|u_f|^2 u_f + 2|u_d|^2 u_f \right) \qquad (3.3)$$

$$\frac{\partial u_d}{\partial z} + \frac{\alpha_d}{2} u_d + \delta \frac{\partial u_d}{\partial T} + \frac{i\beta_{2d}}{2} \frac{\partial^2 u_d}{\partial T^2} = i\gamma_d \left(|u_d|^2 u_d + 2|u_f|^2 u_d \right). \qquad (3.4)$$

We use the subscripts d and f to label the material properties α, β_2, and γ for data and frequency channels, respectively. The term $\delta \partial u_d/\partial T$ in Eq. 3.4 appears due to the group velocity difference between the data channel and the frequency signal. We also have two extra terms, $u_f^2 u_d^* \exp(i\Delta\omega t)$ and $u_d^2 u_f^* \exp(-i2\Delta\omega t)$, which serve as the four-wave mixing terms.

In this chapter we will describe each of the impairment terms in Eqs. 3.3 and 3.4, and we will give suitable conditions under which they can be neglected when calculating the phase stability. We will then show that cross-

phase modulation is the primary optical source of phase instability.

3.2 Optical Impairments

In the previous section, we showed how the nonlinear term creates multiple nonlinear terms. In this section, we describe how each of the terms relates to an optical impairment and how that impairment affects the frequency signal. In the analysis, we discuss conditions under which many of the optical impairments become negligible.

3.2.1 Attenuation and Amplified Spontaneous Emission (ASE) Noise

Attenuation appears in the decoupled equations above as

$$\frac{\partial u_f}{\partial z} = -\frac{\alpha_f}{2} u_f, \qquad \frac{\partial u_d}{\partial z} = -\frac{\alpha_d}{2} u_d. \tag{3.5}$$

The attenuation is due to absorption and scattering and will decrease the optical power of the frequency signal exponentially. Amplifiers are spaced periodically to compensate for the loss of optical power, but they add amplified spontaneous emisssion (ASE) noise due to spontaneous emission of photons. ASE noise is accurately described over the bandwidth of an optical signal as a white noise source with noise power [12]

$$\sigma^2_{ASE} = n_{sp} h \nu_0 (G-1) \Delta\nu, \tag{3.6}$$

where n_{sp} is called the spontaneous emission factor, h is Planck's constant, ν_0 is the center frequency, G is the gain of the amplifier, and $\Delta\nu$ is the bandwidth of the signal.

Consider an optical communication system that has a distance of 800 km and an 80 km amplifier separation operating at the wavelength 1.5 μm with loss $\alpha_{\text{dB}} = 0.2$ dB/km, which implies a gain $G = 40$. A typically amplifier will have a noise figure $n_{\text{sp}} = 2$ with a total of 10 amplifiers. If we suppose that the narrow bandwidth of the frequency signal is on the order of 10 MHz, then the total noise power is 1 nW. If the frequency signal has a power of 1 μW or above, the effect of the noise on the frequency signal will be negligible, while its power is small compared to the power in a data channel, which is typically on the order of 1 mW. Hence, it is possible to simultaneously make the impact of ASE noise on the frequency signal negligible, while ensuring that it does not nonlinearly affect the data channels.

3.2.2 Chromatic Dispersion

The dispersion appears as

$$\frac{\partial u_f}{\partial z} = -\frac{i\beta_{2f}}{2}\frac{\partial^2 u_f}{\partial T^2}, \qquad \frac{\partial u_d}{\partial z} = -\frac{i\beta_{2d}}{2}\frac{\partial^2 u_d}{\partial T^2}. \tag{3.7}$$

This impairment leads to pulse spreading of the optical signal, because its frequency components travel at different velocities. The time spread due to

dispersion is [12]

$$\tau_{\text{disp}} = -\frac{2\pi c}{\lambda^2}\beta_{2f} L \Delta\lambda \tag{3.8}$$

where L is the length of the fiber, and $\Delta\lambda$ is the range of wavelengths. For the optical communication system in the previous example and the frequency signal centered at a wavelength $\lambda \approx 1.5\ \mu$m, we find $\tau_{\text{disp}} = 1$ ps. By contrast, the time slot of a single bit at 10 Gbps occupies 100 ps; so, dispersion can be neglected.

3.2.3 Self-Phase Modulation (SPM)

The terms

$$\frac{\partial u_f}{\partial z} = i\gamma_f |u_f|^2 u_f, \qquad \frac{\partial u_d}{\partial z} = i\gamma_d |u_d|^2 u_d \tag{3.9}$$

correspond to self-phase modulation. This distortion takes the form of a phase shift dependent on the signal power. Thus, linear attenuation limits the effect over some length after each amplifier. The effective length is $L_{\text{eff}} = (1/\alpha)[1 - \exp(-\alpha L)]$, so that $L_{\text{eff}} \approx 20$ km for $\alpha_{\text{dB}} = 0.2$ dB/km.

The maximum phase shift due to self-phase modulation for a length of fiber between amplifiers is [13]

$$\phi_{\text{SPM}} = \gamma P_f L_{\text{eff}}, \tag{3.10}$$

where P_f is the power of the frequency signal. The total maximum phase shift is given by Eq. 3.10 multiplied by the number of amplifiers in the fiber

link.

For our typical system, $\gamma = 1.3$ W^{-1}km^{-1}, $L_{\text{eff}} = 20$ km. If we impose an upperbound on ϕ_{SPM} of 1 radian, then the upper bound on the frequency signal power is 3.8 mW.

3.2.4 Four-Wave Mixing (FWM)

The terms

$$i\gamma_f u_d^2 u_f^* \exp(-i2\Delta\omega t), \qquad i\gamma_d u_f^2 u_d^* \exp(i\Delta\omega t), \tag{3.11}$$

correspond to four-wave mixing. For any two data signals centered at ω_1 and ω_2 with corresponding wavenumbers $\beta(\omega_1)$ and $\beta(\omega_2)$, four-wave mixing (FWM) creates a parasitic wave whenever $\omega_1+\omega_2 = 2\omega_f$ and $\beta(\omega_1)+\beta(\omega_2) = 2\beta(\omega_f)$. This phase-matching condition is avoidable as long as the channels are located away from the zero-dispersion wavelength of the fiber. Placing the frequency signal greater than 5 times its bandwidth away from the zero-dispersion wavelength will eliminate this impairment.

3.2.5 Cross-Phase Modulation (XPM)

The remaining terms,

$$\frac{\partial u_f}{\partial z} = i2\gamma_f |u_d|^2 u_f, \qquad \frac{\partial u_d}{\partial z} = i2\gamma_d |u_f|^2 u_d$$

correspond to cross-phase modulation (XPM), which leads to cross-talk between two channels. This effect becomes negligible when the group velocity

difference between the data channel and frequency signal is large, which occurs when the two signals are spaced far apart in the frequency spectrum. Therefore, the effects of XPM on the frequency signal only has to be computed for the two neighboring data channels. Since our goal is to place the frequency signal between two data channels, XPM is the primary source of frequency distortion. The limitation on the optical power of the frequency signal ($\ll 1$ mW) implies that the effect of XPM due to the frequency signal on the data channels can be neglected.

3.3 Phase noise on the frequency signal

Applying the limits on the system parameters that we have obtained, Eqs. 3.3 and 3.4 simplify to the following equations,

$$\frac{\partial u_f}{\partial z} = i2\gamma_f |u_d|^2 u_f \tag{3.12}$$

$$\frac{\partial u_d}{\partial z} + \frac{\alpha_d}{2} u_d + \delta \frac{\partial u_d}{\partial T} + \frac{i\beta_{2d}}{2} \frac{\partial^2 u_d}{\partial T^2} = i\gamma_d |u_d|^2 u_d. \tag{3.13}$$

The frequency signal has no effect on the data channel, and the equation for the frequency signal becomes linear and is only affected by the power in the data channel. Suppose the frequency signal is of the form $u_f(z,T) = u_f(0,T)\exp[i\phi(z,T)]$, where $u_f(0,T)$ is the initial frequency source and $\phi(z,T)$ is phase distortion due to XPM. We can then solve for the phase distortion

using Eq. 3.12, and we find

$$\phi(z,T) = 4\gamma \int_0^z |u_d(0, T - \zeta\delta)|^2 d\zeta. \tag{3.14}$$

The frequency signal is equally spaced between two neighboring data channels, so Eq. 3.14 has a factor of 4 in front instead of 2.

The data channel is subject to the effects of loss, dispersion, a time shift due to the group velocity difference from the frequency signal, and self-phase modulation. The phase distortion of the frequency signal depends entirely on the evolution of the data channel as it propagates through the fiber.

3.4 Chapter Remarks

By limiting the frequency signal's optical power and its location on the frequency spectrum, we can limit the causes of phase distortion due to optical impairments. As a consequence, the distortion will be due to XPM. In the next chapter, we perform computations to estimate $\phi(z,T)$ using typical system parameters for a commercial fiber optic communication system.

Chapter 4: Results

4.1 Introduction

In the previous chapter, we described limitations on the parameters of a commercial optical communication system and a frequency signal that would limit the distortion of the frequency signal located between two data channels in a commercial wavelength division multiplexed communication system, as shown in Fig. 4.1. The result was a phase distortion due to XPM, given by Eq. 3.14.

It follows that the phase distortion depends on the length of fiber, the relative velocity difference between the frequency signal and the data chan-

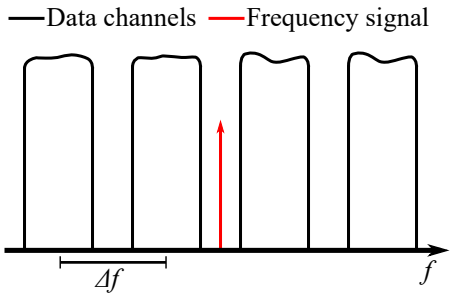

Figure 4.1: Desired frequency domain placement of the frequency signal

nels, and the power of the data channel as it changes over the course of its propagation. We will now vary these parameters and investigate their effect on the frequency stability of the frequency signal.

We choose values for the data channel power and Kerr nonlinearity γ that are typical in commercial optical communication systems. These values are chosen to minimize nonlinear distortion in the data channels [12, 13]. Hence, we may neglect the nonlinear distortion of the data channels when calculating $\phi(z,t)$ and focus on the effect of dispersion. The evolution of the data channel is then easily obtained in the Fourier domain, and we find

$$u_d(0, T - z\delta) = \frac{1}{2\pi}\int_{-\infty}^{\infty} U_d(0,\omega')\exp\left(-\frac{\alpha}{2}z + i\delta\omega' z + \frac{i}{2}\beta_2\omega'^2 z - i\omega' t\right)d\omega', \tag{4.1}$$

where $U_d(0,\omega)$ is the Fourier spectrum of the data channel at $z = 0$ defined as

$$U_d(0,\omega) = \int_{-\infty}^{\infty} u_d(0,t')\exp(i\omega t')dt'. \tag{4.2}$$

We begin by investigating the distribution of the power of the data channel, $|u_d|^2$, as a function of length z. The on-off-keyed symbols of the data channel change over the length of the fiber due to dispersion, self-phase modulation, and attenuation. We first study a system in which attenuation is neglected. We then add the effect of attenuation. Finally, we study the system behavior as the group velocity difference and the data channel power varies.

4.2 Simulation Parameters

The simulation data signal is a $2^{10} - 1$ pseudorandom binary string [28] that is on-off key modulated with optical power of 1 mW with periodic boundary conditions. The fiber has an attenuation of 0.2 dB/km, group velocity dispersion $\beta_2 = -22$ ps^2/km, and Kerr nonlinearity 1.3 W^{-1}km^{-1}. The data channel has a central wavelength of 1530 nm with group velocity difference $\delta = 1$ ps/km relative to the frequency signal. Some of these parameters will vary in the following sections as we study the changes in the XPM-induced phase distortion.

4.3 Without Attenuation

We first neglect attenuation to give us a baseline against which to determine the effect of attenuation.

During propagation, the optical power in each bit of the data channel spreads outside of its time slot into the time slots of its neighbors. After some long distance, the expected power in each time slot will become the same. Therefore, the variance of the data signal's optical power will approach a limit as a function of fiber length. Figure 4.2 shows the data channel power variance over 800 km. Since there is no attenuation, the mean of the data channel power is fixed.

The phase shift ϕ grows as a function of distance because at every propagation length the two channels have some cross-talk which keeps accumu-

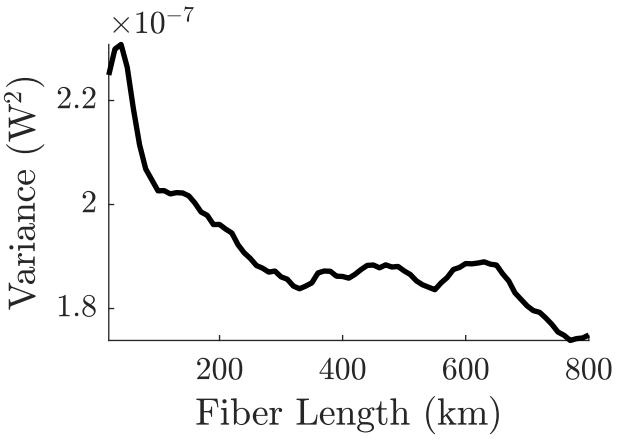

Figure 4.2: Data channel optical power variance vs. fiber length

lating. Figures 4.3a and 4.3b show the mean and variance of the phase distortion due to XPM respectively. The mean of ϕ grows linearly with re-

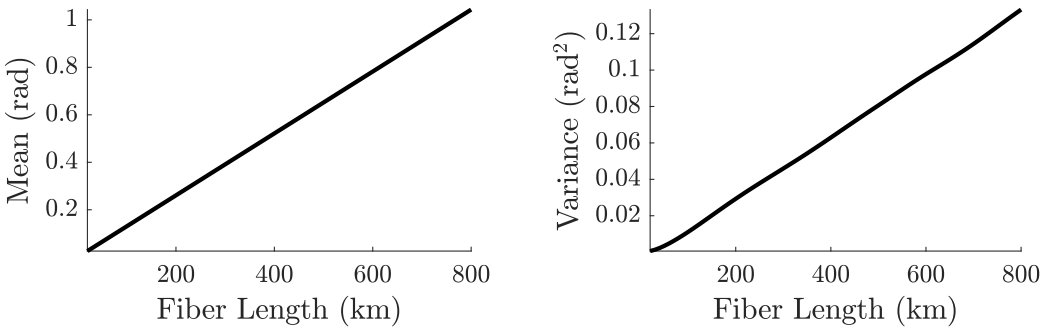

Figure 4.3: (a) Mean of ϕ vs. fiber length (b) Variance of ϕ vs. fiber length

spect to the fiber length because without attenuation, the average energy in the data channel is constant. As a consequence, the mean additive phase error that can be compensated.

We will quantify the phase stability using the measures that we introduced

in Chapter 2. We first consider the first structure equation, $D_\phi^{(1)} = \langle[\phi(t+\tau) - \phi(t)]^2\rangle$, which represents the mean phase accumulation. The structure functions are related to the autocorrelation. A typical data transmission will be a collection of random bits that are uncorrelated with eachother. As the data signal propagates through the fiber, the optical energy associated with each bit occupies a larger amount of time due to dispersion, so that the amount of time in which a bit is correlated with itself increases. Figure 4.4 shows $D_\phi^{(1)}$ at different lengths. The phase stabilizes after a short amount of

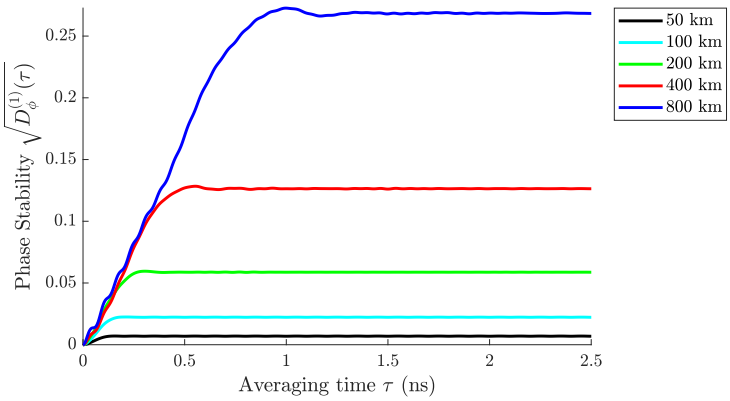

Figure 4.4: Phase Stability vs. averaging time τ

time.

Figure 4.5 shows the Allan deviation. After a short amount of time, the short-term frequency errors are averaged out at the peak, then the Allan Deviation drops off at the rate of τ^{-1}. This fall off continues indefinitely because there are no long-term frequency errors from XPM. We have compute over a short time interval due to memory limitations, but we can use a linear

fit for the τ^{-1} region to determine the Allan Deviation for usual averaging times. At $\tau = 1$ s ADEV $= 3 \times 10^{-15}$, and at $\tau = 10^3$ s ADEV $= 3 \times 10^{-18}$.

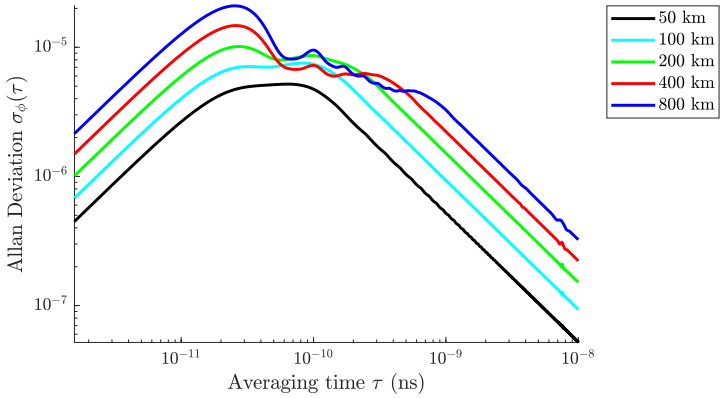

Figure 4.5: Allan Deviation

4.4 Effect of Attenuation

We include the effect of attenuation. We expect the results to be bounded above by the phase and frequency stability without attenuation because the effective length before the nonlinearity, and hence XPM, becomes negligible is 20 km after each amplifier.

First, we compare the variance of the attenuated data channel with the variance without attenuation. Figure 4.6 shows the data channel's optical power variance. Spikes occur every 80 km, corresponding with the locations of the amplifiers.

The mean and variance of ϕ must also grow over the length of the fiber, but they no longer grow almost linearly due to the power variation. Instead,

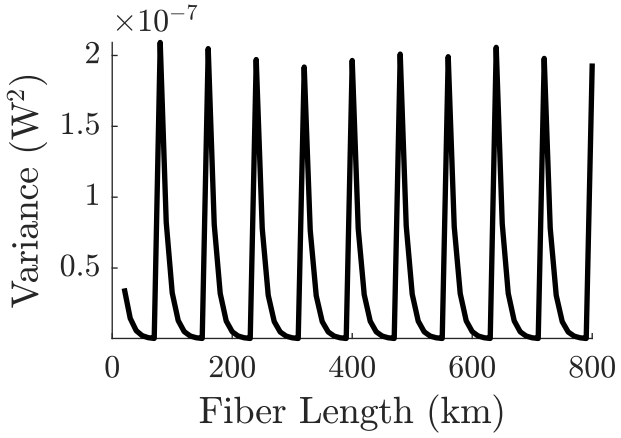

Figure 4.6: Data channel optical power variance vs. fiber length

the mean and the variance grow in steps. Figures 4.7a and 4.7b show the mean and variance of ϕ respectively, in which flat regions where the data channel power is low are visible. The mean and variance are less than those that we obtained when attenuation was neglected.

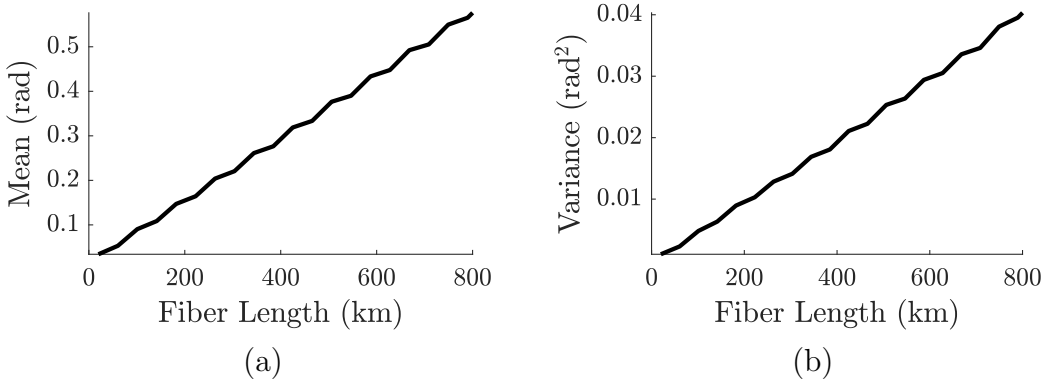

Figure 4.7: (a) Mean of ϕ vs. fiber length (b) Variance of ϕ vs. fiber length

The phase stability $D_{\phi}^{(1)}$ reach an asymptotic value as was the case when attenuation is neglected. Since the asymptotic value depends on the pulse

spreading due to dispersion, the asymptotes occur at the same times. However, the phase stability will be less due to attenuation. Figure 4.8 shows $D_{\phi}^{(1)}$ for different fiber lengths.

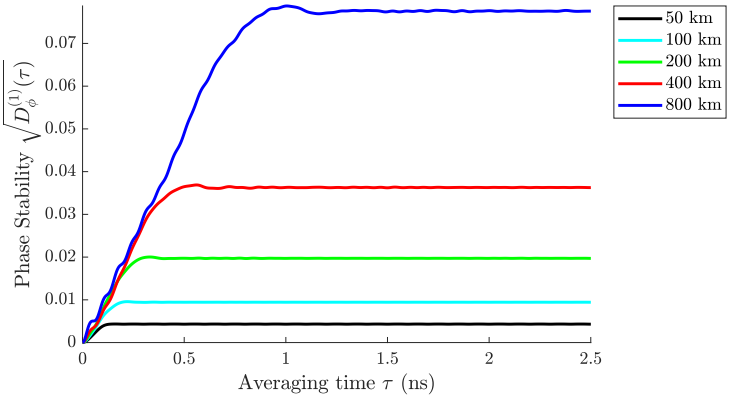

Figure 4.8: Phase stability with attenuation

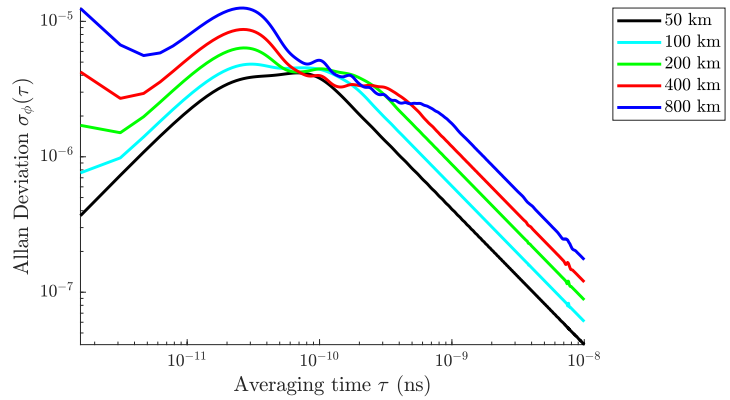

Figure 4.9: Allan Deviation with attenuation

Finally, the Allan deviation will be comparable to the results in the previous section. Figure 4.9 shows the Allan Deviation for several fiber lengths, the bump at the early time intervals corresponds with larger short term frequency errors, but they quickly average out, and, once again, there are no long-term frequency errors. The Allan Deviation will continue to decrease at a rate of τ^{-1}. At $\tau = 1$ s ADEV $= 10^{-15}$, and at $\tau = 10^3$ s ADEV $= 10^{-18}$.

4.5 Varying the Group Velocity Difference

The relative group velocity difference governs the rate at which the data signal travels through a fixed time point in the frequency signal. The group velocity difference is related to the separation between the center frequencies of the data channels and the frequency signal. The value $\delta = (v_f - v_d)/(v_f v_d) =$ 1 ps/km was chosen because it corresponds to the smallest group velocity difference $(v_f - v_d)$ while adhering to the ITU grid standard. As the distance between the center frequencies decreases, the group velocity difference decreases and thus δ decreases. Figure 4.10 shows the phase stability for different relative group velocity differences.

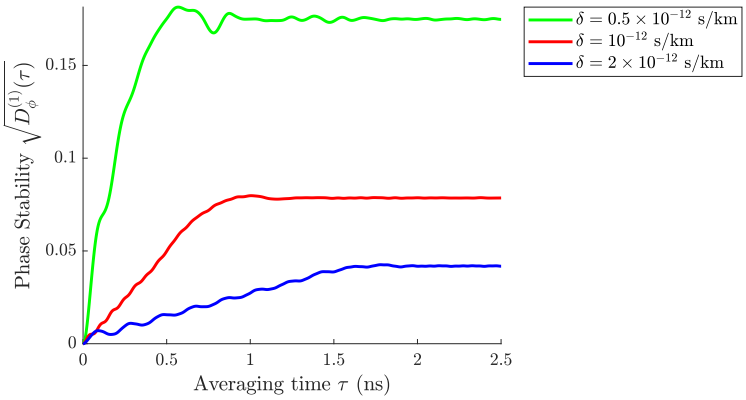

Figure 4.10: Phase stability vs. group velocity difference

4.6 Chapter Remarks

Since the bits of any data channel are uncorrelated, the phase stability will asymptote at an averaging time corresponding to the duration of a bit window and the relative group velocity of the data channel. When the relative group velocity is greater, the asymptote occurs sooner because the data channel passes through a fixed time point at a much greater rate.

The Allan Deviation represents the amount of frequency error. Experiments performing frequency transfer with a frequency signal and data channel located on the ITU standards have Allan Deviation values comparable to our simulated values [8, 10]. The source of error in the experiments is due to temperature. So we see that moving the frequency signal in the interstices of two data channels gives a frequency error on the order of environmental effects.

Chapter 5: Conclusion

A frequency signal in an optical fiber suffers optical impairments due to the medium. By placing requirements on the location and optical power of the frequency signal, we can eliminate a majority of the impairments.

Systems performing frequency transfer over optical fiber place the frequency signal at a center frequency designated for a data channel which uses a large amount of bandwidth. We can solve this issue by putting a frequency signal between two data channels. However, placing the frequency signal closer to the data channels will increase the amount of cross-talk, which causes an increased amount of phase and frequency error.

We computed the amount of frequency error due to cross-talk using the Allan Deviation and found that it was comparable to environmental effects. Hence, it is feasible to place a frequency signal between two data channels on the ITU grid without a significant increase in errors due to cross-phase modulation.

5.1 Future Work

In our work to date, we did not take into account self-phase modulation (SPM) of the data channels. The parameters in modern communication systems are chosen to minimize the impact of SPM, and its largest effect is on the phase of a data channel, which ahs no impact on the frequency signal. Hence, its neglect is reasonable. Moreover, it is difficult computationally to study since we can no longer use Fourier transforms of the input data signal to compute its effect, but must solve the nonlinear Schrödinger equation using a propagation code. Nonetheless, a careful investigation of its effect should be carried out, at a future time.

Bibliography

[1] A. D. Ludlow and J. Ye, "Progress on the optical lattice clock," *Comptes Rendus Physique*, vol. 16, no. 5, pp. 499–505, 2015.

[2] F. Riehle, "Towards a redefinition of the second based on optical atomic clocks," *Comptes Rendus Physique*, vol. 16, no. 5, pp. 506–515, 2015.

[3] S. A. Diddams, "Standards of Time and Frequency at the Outset of the 21st Century," *Science*, vol. 306, no. 5700, pp. 1318–1324, 2004.

[4] D. W. Allan, N. Ashby, and C. C. Hodge, "The science of timekeeping," *Hewlett Packard application note 1289*, pp. 1–88, 1997.

[5] D. Allan and M. Weiss, "Accurate Time and Frequency Transfer During Common-View of a GPS Satellite," *34th Annual Symposium on Frequency Control*, no. May, pp. 334–346, 1980.

[6] D. B. Sullivan, J. C. Bergquist, J. J. Bollinger, R. E. Drullinger, W. M. Itano, S. R. Jefferts, W. D. Lee, D. Meekhof, T. E. Parker, F. L. Walls,

and D. J. Wineland, "Primary atomic frequency standards at NIST," *J. Res. Natl. Inst. Stand. Technol.*, vol. 106, no. 1, pp. 47–63, 2001.

[7] C. Audoin and J. Vanier, "Atomic frequency standards and clocks," *Journal of Physics E: Scientific Instruments*, 1976.

[8] E. Cantin, N. Quintin, F. Wiotte, C. Chardonnet, A. Amy-Klein, and O. Lopez, "Progress on the REFIMEVE+ project for optical frequency standard dissemination," in *Frequency and Time Forum and IEEE International Frequency Control Symposium (EFTF/IFC), 2017 Joint Conference of the European*, pp. 378–380, IEEE, 2017.

[9] K. Turza, A. Binczewski, and W. Bogacki, "Time and frequency transfer in modern DWDM telecommunication networks," pp. 368–370, 2017.

[10] J. Serrano, M. Lipinski, T. Wlostowski, E. Gousiou, E. van der Bij, and M. Cattin, "The White Rabbit project," in *2nd International Beam Instrumentation Conference*, p. THBL2, 2013.

[11] P. Krehlik, L. Sliwczynski, J. Dostal, J. Radil, V. Smotlacha, and R. Velc, "CLONETS - Clock network services: Strategy and innovation for clock services over optical-fibre networks," *International Conference on Transparent Optical Networks*, vol. Part F81-E, no. 2008, pp. 1–2, 2017.

[12] G. P. Agrawal, *Fiber-Optic Communication Systems*. Wiley Series in Microwave and Optical Engineering, Wiley, 2012.

[13] G. P. Agrawal, *Nonlinear fiber optics*. Academic Press, 2013.

[14] C. R. Menyuk, "Transmission of a frequency channel through a long-haul optical fiber communications link," in *2015 Joint Conference of the IEEE International Frequency Control Symposium the European Frequency and Time Forum*, pp. 736–741, April 2015.

[15] ITU-T, "G.694.1 (02/2012), Spectral grids for WDM applications: DWDM frequency grid," *Series G.694.1*, pp. 1–16, 2012.

[16] J. G. Proakis, *Digital Communications*. Electrical engineering series, McGraw-Hill, 2001.

[17] B. E. Blair, *Time and Frequency: Theory and Fundamentals*. No. no. 140 in Monograph, U.S. National Bureau of Standards, 1974.

[18] Ł. Śliwczyński, P. Krehlik, and M. Lipiński, "Optical fibers in time and frequency transfer," *Measurement Science and Technology*, vol. 21, no. 7, p. 75302, 2010.

[19] Ł. Śliwczyński and P. Krehlik, "Multipoint joint time and frequency dissemination in delay-stabilized fiber optic links," *IEEE Transactions on Ultrasonics, Ferroelectrics, and Frequency Control*, vol. 62, no. 3, pp. 412–420, 2015.

[20] P. Kartaschoff, *Frequency and Time*. New York: Academic Press, 1978.

[21] D. W. Allan, J. H. Shoaf, and D. Halford, "Statistics of Time and Frequency Data Analysis," in *Time and Frequency: Theory and Fundamentals* (B. E. Blair, ed.), p. 151, 1974.

[22] W. J. Riley, *Handbook of Frequency Stability Analysis*, vol. 31. 1994.

[23] J. Rutman, "Oscillator Specifications: A Review of Classical and New Ideas," *31st Annual Symposium on Frequency Control. 1977*, pp. 291–301, 1977.

[24] W. C. Lindsey, "Theory of Oscillator Instability Based Upon Structure Functions," *Proceedings of the IEEE*, vol. 64, no. 12, pp. 1652–1666, 1976.

[25] W. Loh, S. Yegnanarayanan, R. J. Ram, and P. W. Juodawlkis, "Unified theory of oscillator phase noise I: White noise," *IEEE Transactions on Microwave Theory and Techniques*, vol. 61, no. 6, pp. 2371–2381, 2013.

[26] W. Loh, S. Yegnanarayanan, R. J. Ram, and P. W. Juodawlkis, "Unified theory of oscillator phase noise II: Flicker noise," *IEEE Transactions on Microwave Theory and Techniques*, vol. 61, no. 12, pp. 4130–4144, 2013.

[27] E. O. Schulz-DuBois and I. Rehberg, "Structure function in lieu of correlation function," *Applied Physics*, vol. 24, no. 4, pp. 323–329, 1981.

[28] F. J. MacWilliams and N. J. A. Sloane, "Pseudo-random sequences and arrays," *Proceedings of the IEEE*, vol. 64, no. 12, pp. 1715–1729, 1976.